Physica B 423 (2013) 16–20

Contents lists available at SciVerse ScienceDirect

Physica B

journal homepage: www.elsevier.com/locate/physb

Comparison of the electronic band profiles and magneto-optic properties of cubic and orthorhombic $SrTbO_3$

Zahid Ali [a,*], Imad Khan [a], Iftikhar Ahmad [a], S. Naeem [b], H.A. Rahnamaye Aliabad [c], S. Jalali Asadabadi [d], D. Zhang [e]

[a] Materials Modeling Center, Department of Physics, University of Malakand, Chakdara, Pakistan
[b] Department of Physics, Islamia College University, Peshawar, Pakistan
[c] Department of Physics, Hakim Savzevari University, Sabzevar, Iran
[d] Department of Physics, Faculty of Science, University of Isfahan, Hezar Gerib Avenue, Isfahan 81744, Iran
[e] Department of Physics, California State University, Fresno, USA

ARTICLE INFO

Article history:
Received 20 December 2012
Received in revised form
15 April 2013
Accepted 17 April 2013
Available online 2 May 2013

Keywords:
Perovskites oxides
DFT
Electronic band profiles
Semiconductivity
Magnetism
Optical properties

ABSTRACT

The all electrons full potential linearized augmented plane waves (FP-LAPW) method with GGA+U is used to study $SrTbO_3$ perovskite in cubic and orthorhombic phases. The structural parameters and ground state magnetic properties are found consistent with the experimental results. The electronic band structures and density of states demonstrate that $SrTbO_3$ is a wide band gap semiconductor in both phases. The magnetic studies of the material show that the nature of the compound is G-type anti-ferromagnetic. The calculated magnetic moment of Tb^{+4} is found consistent with the experiments. Furthermore, the optical properties demonstrate that the optical gap of the material is 1.8 eV, which lies in the visible region of the electromagnetic spectrum and hence the compound can be used in optoelectronic devices.

1. Introduction

Perovskite oxides are the most commonly occurring important materials. These oxides have always been the focus of studies because of their simple synthesis and diverse physical properties. Some of these oxides are integral part of many established high-tech devices [1–3]. These materials are commonly used in chemical reactors, solid state fuel cells, gas separation membranes, high temperature superconductors (HTSC), optoelectronic devices and magnetoelectronic technologies [4,5]. One of the important members of this family of oxides is $SrTbO_3$.

The synthesis of $SrTbO_3$ is reported by the standard solid state reaction of two materials $SrCO_3$ and Tb_4O_7 [6]. The experimental studies of Hojezyk et al. [7] reveal cubic structure of the compound. They are of the opinion that this compound could be a potential candidate for high temperature superconductor devices. This compound exists in cubic [7] and orthorhombic [6,8] structures with space group Pm-3 m (no. 221) and Pnma (no. 62) respectively. The experimentally measured as well as calculated lattice constant of the cubic $SrTbO_3$ is 4.18 Å [7,9–11].

$SrTbO_3$ shows anti-ferromagnetic transition at 30.5 K, and above 60 K the susceptibility chases the Curie-Weiss law. The compound possesses G-type anti-ferromagnetic behavior with effective magnetic moment of $7.96\mu_B$ [7]. Tezuka et al. [8] reported in their experimental studies that the magnetic moment of Tb^{+4} is $6.76\mu_B$ in orthorhombic phase with G-type anti-ferromagnetic nature.

The aim of this theoretical work is to study and compare the ground state structural parameters and geometry, electronic behavior, stable magnetic phase and optical properties of the cubic and orthorhombic $SrTbO_3$. All the calculations are performed with the full potential linearized augmented plane waves (FP-LAPW) method with the exchange correlation of Perdew–Burke–Ernzerhof generalized gradient approximation with the inclusion of the Coulomb interaction U (PBE-GGA+*U*).

2. Computational details

The Kohn–Sham equations [12] are solved to calculate the ground state physical properties like structural parameters, electronic, magnetic and optical behavior of $SrTbO_3$ perovskite in cubic and orthorhombic phases. The particulars of the spin-polarized

* Corresponding author. Tel.: +92 333 902 7401.
E-mail address: zahidf82@gmail.com (Z. Ali).

0921-4526/$ - see front matter © 2013 Elsevier B.V. All rights reserved.
http://dx.doi.org/10.1016/j.physb.2013.04.041

FP-LAPW technique, formulas and the WIEN2k software used in the present work can be found in Ref. [13].

In order to calculate the electronic behavior as well as magnetic and optical properties of the $SrTbO_3$ by GGA+U, it is assumed that the density matrix is diagonal and U is the same for all Coulomb interactions ($U_{ij}\equiv U$) and J is also the same for all exchange interactions ($J_{ij}\equiv J$). There are several ways to incorporate the U-term [14,15] but here the self-interaction correction (SIC) introduced by Anisimov and his coworkers [16] as implemented in the WIEN2k package is used. In the GGA+U^{SIC} method the total energy is

$$E = E_0 + E_{GGA+U^{SIC}} \quad (1)$$

In Eq. (1), E_0 is defined to be $T_{S,0} + E_{ei} + E_H + E_{ii} + E_{XC}$, where $T_{S,0}$, E_{ei}, E_H, E_{ii} and E_{XC} are the kinetic energy, Coulomb electron–nuclei interaction, Hartree energy, nuclei–nuclei Coulomb interaction and exchange-correlation energy respectively. Where,

$$E_{GGA+U^{SIC}} = \frac{U-j}{2}(N-\sum_{m,\sigma} n^2_{m,\sigma}) \quad (2)$$

In Eq. (2), N is for the total number of electrons and $n_{m,\sigma}$ is the occupation number of $|l,m,\sigma\rangle$ state with spin σ. An approximated correction value of U–J for the SIC is probably the best for strongly correlated systems and, as recommended in Ref. [13], for a full potential method we use an "effective" $U_{eff}=U-J$ by setting $J=0$.

After examining and testing several values of Hubbard potential in order to adjust the Tb-4f orbitals level in the density of states for $SrTbO_3$, different values of U_{eff} (0, 2, 4, 6 eV) are used in order to treat the 4f state of Tb correctly and the final Hubbard potential used is $U_{eff}=U-J=4.0$ eV for U.

The core electrons are treated fully relativistically and the valence electrons are treated semi-relativistically. In order to ensure that no electron leakage is taking place semi-core states are included so that accurate results can be achieved; 2300 k-points are used and $K_{max}/R_{MT}=8.00$ determines the plane wave basis functions.

3. Results and discussion

3.1. Ground state structural properties

$SrTbO_3$ have been studied in cubic and orthorhombic phases in order to explore the ground state structural properties and magnetic interaction, the energy and volume are optimized and the values are fitted in Birch-Murnaghan equation of state [17]. The ground state magnetic interaction is evaluated by calculating the difference of the total energy of the compound per unit cell. Fig. 1 shows the optimization curves for both phases of the compound. From the ground state volumes the equilibrium structural parameters such as the lattice constants, bulk moduli and ground state energies are obtained. The calculated structural parameters per unit cell for both phases are presented in Table 1. DFT usually underestimates physical quantities. In the present work the calculated lattice constant for the cubic $SrTbO_3$ is 0.95% less than the experimentally measured value [7] and 0.48% less than the analytical reported works [10,11]. Similarly, for orthorhombic phase the lattice constant is 0.52% less than the experimental work [8]. The calculated ground state energies show that orthorhombic phase is more stable than the cubic phase. Furthermore, we calculate the bond lengths between different atoms in both phases and are also presented in Table 1. In cubic phase the bond length Sr O is larger than Tb–O and correspond to $\sqrt{3}/2a_0$ and $1/2a_0$ respectively. The bond length for Tb–O(1) is 2.1382 Å and for Tb–O(2) is 2.139 Å in orthorhombic phase. The bond angles between different atoms in orthorhombic phase Tb–O(1)–Tb and

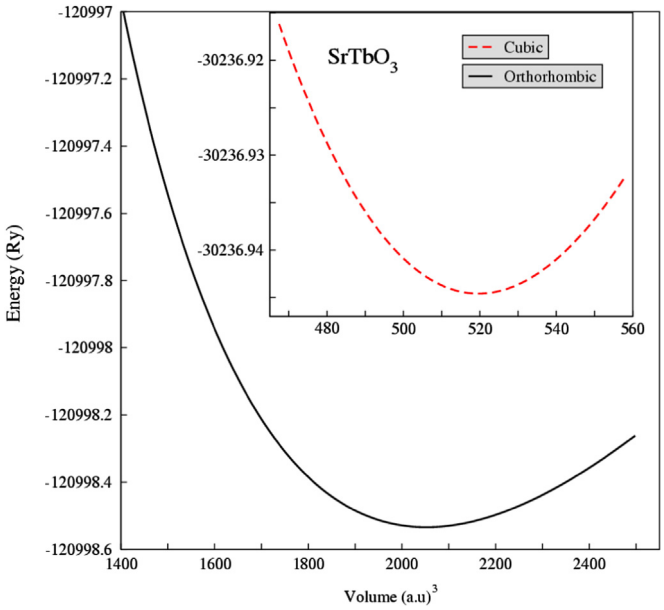

Fig. 1. Optimization curves of $SrTbO_3$ in cubic and orthorhombic phase.

Table 1
Experimental and calculated values of the lattice constants, ground state energies, bulk moduli (B), bond lengths, energy band gaps and magnetic moments of Tb per unit cell of $SrTbO_3$ in cubic and orthorhombic phases.

$SrTbO_3$	Present work	Experimental	Analytical
Cubic			
a_o (Å)	4.16	4.18[a]	4.18[b, c]
E_{FM} (Ry)	−30236.9445		
E_{AFM} (Ry)	−30236.4895		
E_{G-AFM} (Ry)	−30236.9738		
B (GPa)	132.7336		
Bond lengths			
Sr–O (Å)	2.9698		
Sr–Tb (Å)	3.6373		
Tb–O (Å)	2.10		
Band gap			
Spin up (↑) Γ–Γ (eV)	4.4		
Spin down (↓) Γ–Γ (eV)	1.3		
Magnetic properties			
Tb^{+4} (μ_B)	6.50		
Orthorhombic			
a (Å)	5.931	5.962[d]	
b (Å)	8.308	8.351[d]	
c (Å)	5.844	5.874[d]	
B (GPa)	113.476		
E_{FM} (Ry)	−120998.5341		
E_{AFM} (Ry)	−120998.3398		
E_{G-AFM} (Ry)	−120998.5786		
Bond lengths			
Tb–O(1) (Å)	2.1382		
Tb–O(2) (Å)	2.1390		
Bond angles			
Tb–O(1)–Tb (°)	150.26		
Tb–O(2)–Tb (°)	151.27		
Band gap			
Spin up (↑) Γ–Γ (eV)	5.0		
Spin down (↓) Γ–Γ (eV)	1.3		
Magnetic properties			
Tb^{+4} (μ_B)	6.60	6.75[d]	

[a] [7].
[b] [10].
[c] [11].
[d] [8].

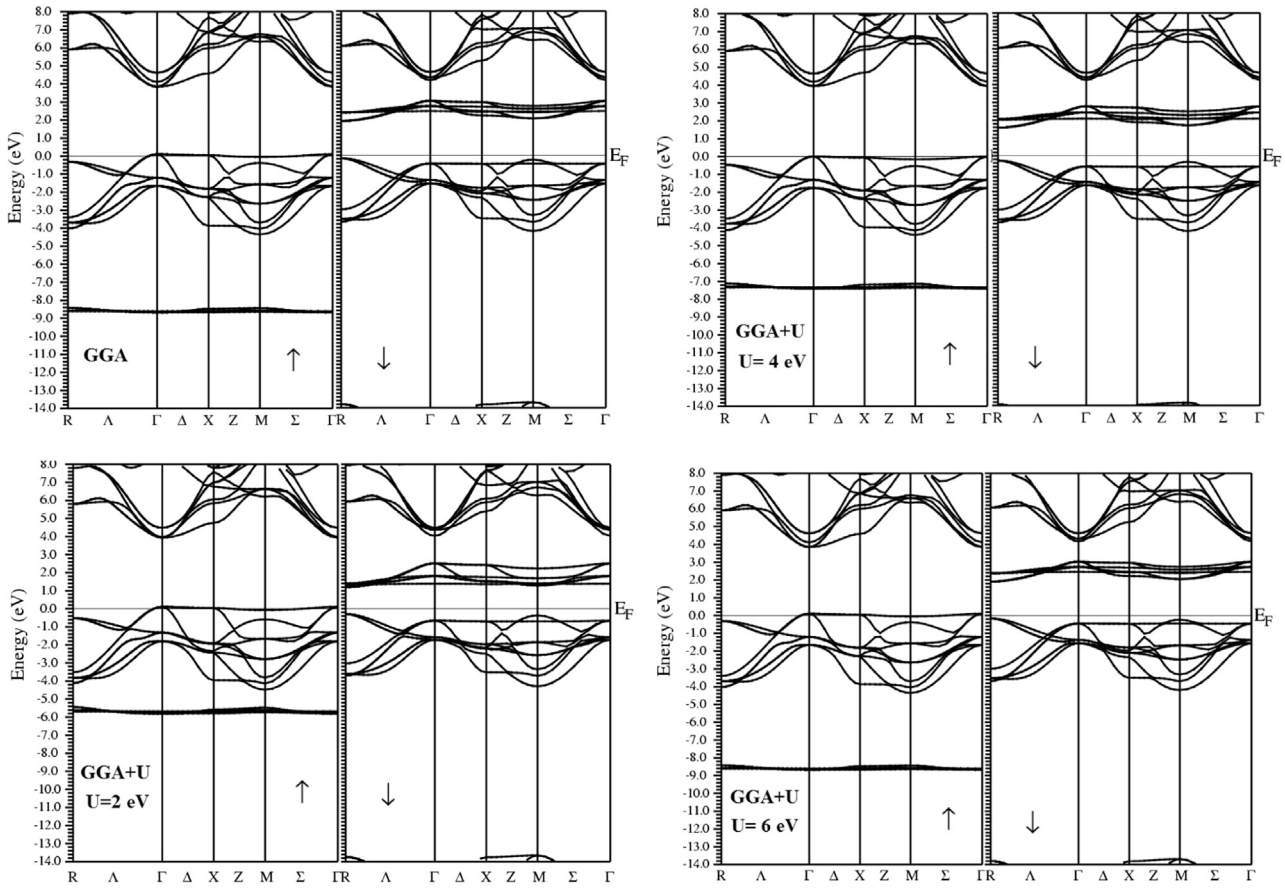

Fig. 2. Spin-polarized electronic band structures of cubic $SrTbO_3$ by GGA+U (U=0, 2, 4, 6 eV).

Tb–O(2)–Tb are 150.26° and 151.27° respectively. These bond lengths and bond angles play important role in the stability of a crystal structure.

3.2. Electronic band structure and density of states

Self consistent field calculations are performed in order to study the electronic properties of $SrTbO_3$ in cubic and orthorhombic phases. The spin polarized electronic band structures of the compound are calculated using GGA with the inclusion of different Coulombic interaction U (U=0, 2, 4 and 6 eV), presented in Fig. 2. It is obvious from the figure that for U=0, in case of spin up state, a wide gap exists (4.1 eV) between the valance and conduction bands at Γ symmetry point, while for the spin down state the gap is stretched and f-state of Tb jumps into conduction band, hence polarization occurs at the Fermi level, but again a gap of 3.1 eV exists at the R symmetry point. It can be seen from the figures that for spin up states the energy gap increases by the application of the Coulomb interaction U up to U=4 eV where the 4f state of Tb is localized, while band gap decreases when U is increased beyond this value as shown for U=6 eV. For U=2 eV in case of spin up state the maxima of the valance band moves backward which increases the gap (4.3 eV) at the same symmetry point. A similar trend is also observed for U=4 eV with a gap of 4.4 eV, whereas for U=6 eV the energy gap is decreased to 4.0 eV. In case of spin down state the gap stretches for U=2 eV (1.34 eV) while no change is observed in details for U=4 and 6 eV. Similar band structures are observed for the orthorhombic phase at U=4 eV (figures are not given). In case of spin up state a wide gap of 5 eV exists between the valance and conduction band, while stretches to 1.3 eV for spin down state.

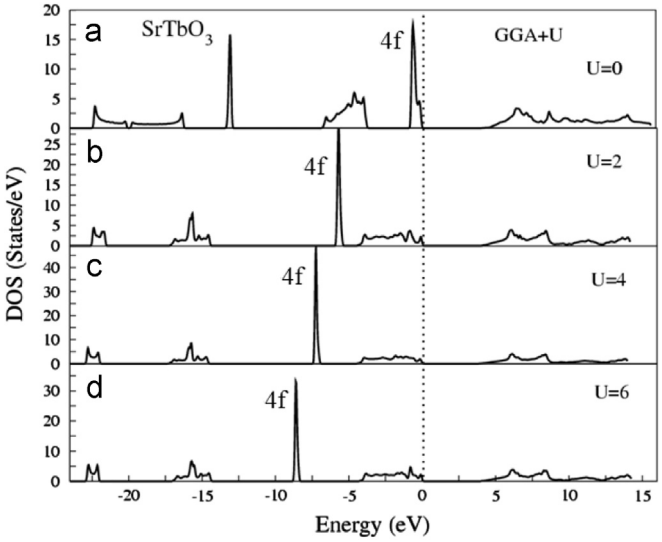

Fig. 3. Total density of states of cubic $SrTbO_3$ by GGA+U (U=0, 2, 4 and 6 eV).

To explain the origin of the electronic band structures, we calculate the total densities of states (DOS) for different values of U, in which energy is scaled with respect to the Fermi level. The calculated densities of states for different values of U for cubic phase are presented in Fig. 3. It is obvious from the figure that in case of simple GGA (U=0) the f-state of Tb lies near the Fermi level at −0.67 eV in the valance band. When calculations are performed with the insertion of the Coulomb interaction for U=2 eV the f-state of Tb moves toward the core in the valance band and is

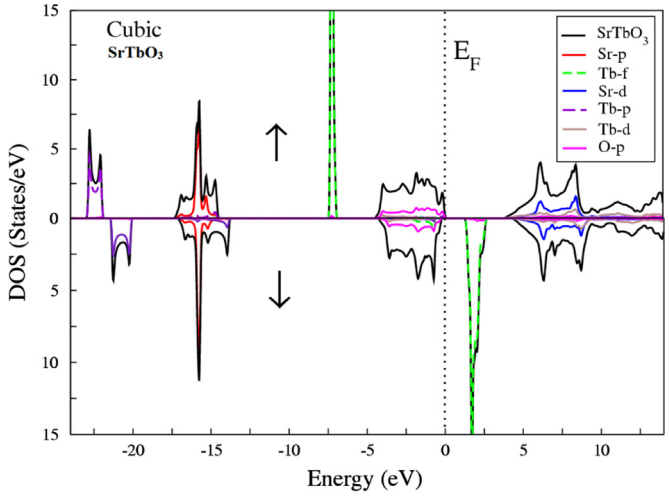

Fig. 4. Spin-polarized total partial density of states of cubic $SrTbO_3$ GGA+U (U=4 eV).

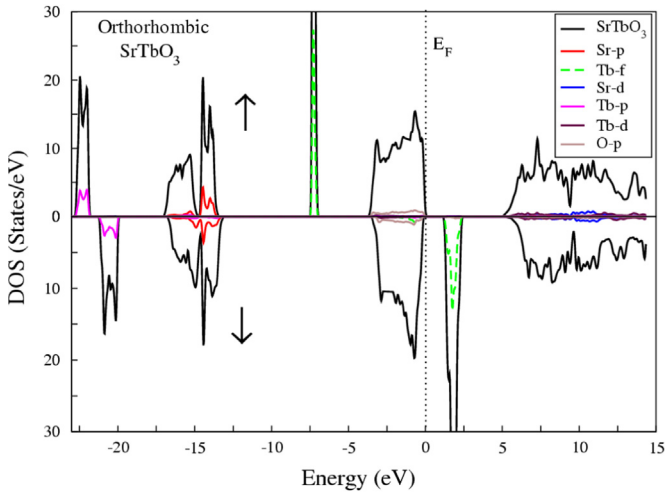

Fig. 5. Spin-polarized total partial density of states of orthorhombic $SrTbO_3$ GGA+U (U=4 eV).

localized at −5.6 eV. For U=4 eV the f-state is further moved and localized at −7.25 eV with a gap of 4.4 eV. On further increasing the U value to 6 eV, the f-state moves downward in the valance band and is localized at −8.6 eV but in this case the energy band gap is decreased (4 eV). Hence the optimized value for U is 4 eV. The calculated spin polarized total and partial DOSs for U=4 eV are presented in Fig. 4. It is obvious from the figure that the bottom of the valance band is occupied by the Tb-5p states in the range −22.9 to −21.9 eV. From −17 to 14.5 eV the contribution of Sr-4p states takes place. Tb-4f state is localized at −7.2 eV in the valance band, while O-2p states density occurs in the range of –4.4 eV to Fermi level. In conduction band the main contribution of Tb-5d and Sr-3d states occur from 4.4 to 14 eV, whereas mixed contribution is due to the unoccupied d states of Sr and Tb (shown in Fig. 4). A wide band gap exists between the valance and conduction band, which makes the material wide band gap semiconductor. For spin down state, the density of Tb-5p state shifts forward in the range −20 to −21.5 eV, while the 2p state of O lie at the same position near the Fermi level. Whereas the 4f-state of Tb jumps into conduction band and is localized at 1.7 eV. A gap still exists between the valance and conduction band for the spin down state of the same compound. Fig. 5 shows the total and partial densities of states of the orthorhombic phase of the compound. Similar results are also observed for orthorhombic phase with a small difference in details. This difference is due to the change in the number of atoms per unit cell. Hence, the spin polarized study reveals that the compound is a wide band gap semiconductor for spin up state and narrow gap for spin down state.

3.3. Magnetic properties

The stable magnetic state of the compound is optimized by calculating the ground state energy per unit cell of the compound in both phases as reported in our previous work [18]. The magnetic ground state properties of the material, favoured G-type anti-ferromagnetic phase in which the compound lowers its ground state energy as compared to the other magnetic states, shown in Table 1. This shows that our theoretical results are consistent with the available experimental results of $SrTbO_3$ [6,8].

Anti-ferromagnetic rare-earth perovskites generally have low temperatures order as compared to those compounds possessing transition metals (TM) elements [19]. Hutchings et al. [20] investigated the exchange coupling in rare-earth actinides for f^7 ions and concluded that the superexchange process is complicated in these rare-earth materials due to the spin-polarization of the 5s and 5p orbitals. As a result, a large number of contributions to the exchange energy have to be included, showing covalency terms involving in 5p electrons of rare-earth elements [21].

The magnetic properties of the compound are examined especially the magnetic moments of Tb^{+4} ion per unit cell. Our calculated magnetic moment of Tb for cubic phase at U=0 eV is 6.29μ_B, which increases by increasing the U up to a certain value and then decreases. For U=2 eV the magnetic moment of Tb^{+4} is 6.44μ_B and for U=4 eV it increases up to 6.5μ_B and then decreases with the increase in U. Similarly for orthorhombic phase the magnetic moment of Tb^{+4} is 6.6μ_B at U=4 eV. The experimentally reported value of the magnetic moment of Tb^{+4} is 6.76μ_B for orthorhombic $SrTbO_3$ [8]. This shows that our calculated value of the magnetic moment is very close to the experimentally reported results.

3.4. Optical spectra

As $SrTbO_3$ has a semiconducting wide band gap nature, so it is predicted that it will be an efficient compound for optoelectronic devices. The frequency dependent optical parameters like dielectric functions, refractive index, reflectivity and energy loss function are calculated in both the phases using GGA+U at U=4 eV. Dielectric functions are used as an investigative tool for the calculation of various optical properties of a material. In Fig. 6, the real part of dielectric function $\varepsilon_1(\omega)$ is plotted for both cubic and orthorhombic crystal structures. From the figure it can be seen that orthorhombic phase has a negligible anisotropy. The important parameter in the real part of dielectric function is $\varepsilon_1(\infty)$ and its value is 5.12. It has two peaks and these peaks correspond to different optical transitions. The first peak is observed at 3.21 eV and the second at 6.23 eV in the cubic phase while in orthorhombic structure they appear at 160 eV and 6.22 eV. For energies larger than 24 eV the real part of dielectric function becomes negative which means that the compound shows metallic behavior. The imaginary part of dielectric function $\varepsilon_2(\omega)$ is shown in Fig. 6. The offset points in all optical axes are observed at 1.80 eV which corresponds to the optical gap of the compound. A wide range of absorption region is observed with two main peaks. The first peak is obtained at 3.41 eV for all the axes while the second one at 7.04 eV for cubic and 8.0 eV for orthorhombic. As the material has wide and direct band gap nature, it could be efficient candidate for visible optoelectronic applications.

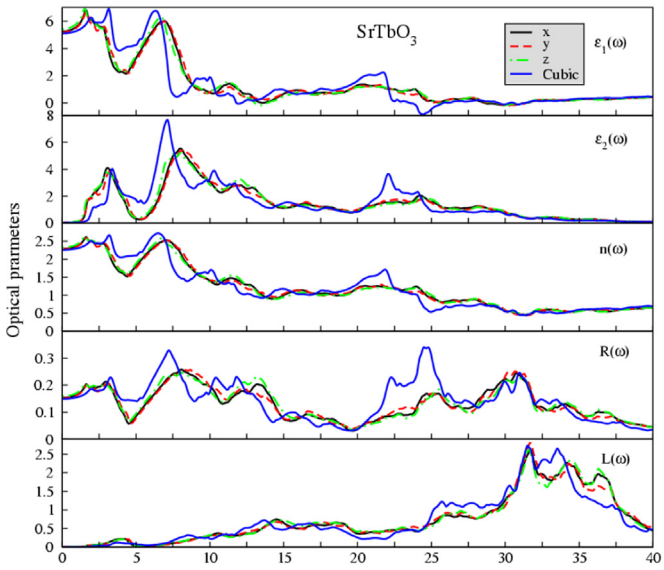

Fig. 6. Different frequency dependent optical parameters dielectric functions, refractive index, reflectivity and energy loss function of cubic and orthorhombic $SrTbO_3$ at (U=4 eV).

The calculated refractive index $n(\omega)$ for $SrTbO_3$ in the energy range 0–40 eV is plotted in Fig. 6. From the figure the zero frequency refractive index is 2.28 and it gradually increases up to the first peak in the form of a hump. The maximum refractive index is found in the direct transition from the valence band to conduction band. After this peak value the refractive index decreases with respect to higher energies, this is due to the fact that higher energy photons are absorbed by the material and the material becomes gradually opaque.

The normal incident reflectivity $R(\omega)$ is calculated for $SrTbO_3$ and plotted in Fig. 6. The minimum reflectivity occurs in the energy range 0–5 eV is due to the collective plasma resonance and the zero frequency limit of reflectivity for $SrTbO_3$ is 0.32%. There are high reflection peaks at energies 7.2 eV and 25 eV corresponding to the negative values of ε_1 (ω).

Electron energy loss spectroscopy (EELS) $L(\omega)$ is a precious tool for the investigations of the different aspects of a material [22]. It provides information about elastically scattered and non-scattered electrons and the number and type of atoms being struck by the beam [23]. Electron energy loss function for $SrTbO_3$ is plotted in Fig. 6. It is obvious from the figure that for a photon with energy less than the band gap of a material no energy loss occurs, which means no scattering happens. In the intermediate energy range inelastic scattering is observed and the loss is maximum, where peak is found at 31.5 eV. This peak in the energy loss spectrum corresponds to plasma resonance and the corresponding frequency is called plasma frequency, above which the material exhibits metallic behavior whereas below that the material has a dielectric property.

4. Conclusions

In summary the perovskite $SrTbO_3$ has been studied theoretically in cubic as well as in orthorhombic phase. The calculations are performed by the all electron full potential linearized augmented plane waves (FP-LAPW) method and employing the PBE-GGA+U with different values of U. The structural parameters are found consistent with the experimental reported work. Electronic band structures and densities of states demonstrate that $SrTbO_3$ is a wide band gap semiconductor. The magnetic studies of the material show that the nature of the compound is G-type antiferromagnetic. The magnetic moment of Tb^{+4} is found in closed agreement with the experiment. Optical properties show that the material is active in visible region. On the basis of these physical properties, it is also concluded that $SrTbO_3$ is a novel optical material operating in visible spectral region of the electromagnetic spectrum.

References

[1] G. Murtaza, I. Ahmad, B. Amin, A. Afaq, M. Maqbool, J. Maqssod, I. Khan, M. Zahid, Opt. Mater. 33 (2011) 553.
[2] Z. Ali, I. Ahmad, A.H. Reshak, Physica B 410 (2013) 217.
[3] Z. Ali, I. Ahmad, B. Amin, M. Maqbool, G. Murtaza, I. Khan, M.J. Akhtar, F. Ghafor, Physica B (2011)3800.
[4] L. Soderholm, S. Skanthakumar, U. Staub, M.R. Antonio, C.W. Williams, J. Alloys Compd. (1997)623.
[5] Z. Ali, I. Ahmad, I. Khan, B. Amin, Intermetallics 31 (2012) 287.
[6] Y. Hinatsu, J. Solid State Chem. 100 (1992) 136.
[7] R. Hojczyk, Chun-Lin Jia, U. Poppe, K. Urban, Phys. C: Superconductivity 282–287 (1997) 731.
[8] K. Tezuka, Y. Hinatsu, Y. Shimojo, Y. Moriiz, J. Phys.: Condens. Matter 10 (1998) 11703.
[9] A. Majid, Y.S. Lee, Adv. Inf. Sci. Serv. Sci. 2 (2010) 3.
[10] R. Ubic, J. Am. Ceram. Soc. 90 (2007) 3326.
[11] L.Q. Jiang, J.K. Guo, H.B. Liu, M. Zhu, X. Zhou, P. Wu, C.H. Li, J. Phys. Chem. Solids 67 (2006) 1531.
[12] W. Kohn, L.S. Sham, Phys. Rev. A 140 (1965) 1133.
[13] P. Blaha, K. Schwarz, G.K.H. Madsen, D. Kvasnicka, J. Luitz, WIEN2K: An Augmented Plane Wave+Local Orbital Program for Calculating Crystal Properties, Techn Universitat, Wien, Austria, 2001.
[14] A.G. Petukhov, I.I. Mazin, Phys. Rev. B 67 (2003) 153106.
[15] P. Novak, J. Kunes, L. Chaput, W.E. Pickett, Phys. Status Solidi B 243 (2006) 563.
[16] V.I. Anisimov, I.V. Solovyev, M.A. Korotin, M.T. Czyzyk, G.A. Sawatzky, Phys. Rev.B 48 (1993) 16929.
[17] F. Birch, Phys. Rev. 71 (1947) 809.
[18] Z. Ali, Iftikhar Ahmad, S. Jalali Asadabadi, Comp. Mat. Sci. 67 (2012) 151.
[19] P.W. Anderson, Phys. Rev. 86 (1952) 694.
[20] M.J. Hutchings, R.J. Birgenau, W.P. Wolf, Phys. Rev. 168 (1968) 1026.
[21] R.E. Watson, A.J. Freeman, Phys. Rev. 156 (1967) 251.
[22] I. Khan, A. Afaq, H.A. Rahnamaye Aliabad, I. Ahmad, Comp. Mat. Sci. 61 (2012) 278.
[23] I. Khan, I. Ahmad, B. Amin, G. Murtaza, Z. Ali, Physica B 406 (2011) 2509.